

ORIGINAL ARTICLE

Open Access

Effect of doping concentration on absorbance, structural, and magnetic properties of cobalt-doped ZnO nano-crystallites

Muhammad Ahsan Shafique¹, Saqlain A Shah^{2*}, Muhammad Nafees¹, Khalid Rasheed^{1,3} and Riaz Ahmad¹

Abstract

Controlled conduction of magnetic spins is desired for data processing in modern spintronic devices. Transition metal-doped ZnO is a potential candidate for this purpose. We studied the effects of cobalt doping on structural, absorbance, and magnetic properties of ZnO nano-particles. Different compositions ($\text{Zn}_{0.99}\text{Co}_{0.1}\text{O}$, $\text{Zn}_{0.97}\text{Co}_{0.3}\text{O}$, and $\text{Zn}_{0.95}\text{Co}_{0.5}\text{O}$) of cobalt-doped ZnO were fabricated using metallic chlorides by co-precipitation method. XRD revealed standard ZnO wurtzite crystal structure without lattice distortion due to impurities but showed presence of additional phases at higher doping ratios. Fourier transformed infrared spectroscopy also confirmed the standard ZnO profiles at lower doping ratios but additional phases at higher doping. Vibrating sample magnetometer showed soft ferromagnetic behavior for low impurity samples and harder ferromagnetic behavior for higher doping at room temperature. A simultaneous differential scanning calorimetry/thermo gravimetric analysis was performed to study the phase variations during crystallization.

Keywords: Cobalt-doped ZnO, DMS, FTIR, VSM, Crystal growth, Metallic chlorides

Background

ZnO is not new for researchers. Its fundamental structural properties were studied in 1935 for the first time by Bunn [1], and then detailed optical studies were carried out by Damen et al. [2] and Decremps et al. [3] using Raman spectroscopy.

Initially, ZnO got the attention of researchers because of its potential applications in laser due to large exciton binding energy (60 meV) and wide band gap about 3.3 eV [4]. Now, ZnO is being studied because of its promising application for spintronics and optoelectronics.

Spintronics requires controlled conduction and high degree of spin polarization. ZnO is a semiconductor in nature and has very favorable structure carrier-induced ferromagnetism. After the theoretical study of Dietl et al. in which they observed room temperature ferromagnetism in Mn-doped ZnO [5], the researchers started a comprehensive study of Mn and other transition metal-doped ZnO. The electronic structure of doped metal is

strongly affected by the electronic structure of host lattice. There is a strong hybridization of 3D-host energy levels and 3D-3D Coulomb interactions [4]. Initially, some researchers reported absence of ferromagnetism at room temperature. Simultaneously, some of them reported room temperature ferromagnetism but in the materials fabricated at low temperatures [6,7]. In our work, Co-doped ZnO nano-particles ($\text{Zn}_{1-x}\text{Co}_x\text{O}$, $x = 1, 3, \text{ and } 7$) were successfully fabricated using chemical co-precipitation method to study the effect of doping concentration on structural, absorbance, thermal, and magnetic properties.

Methods

Experimental procedure

Pure chemicals (99.9%) cobalt chloride ($\text{Co}(\text{Cl})_2$), zinc chloride ($\text{Zn}(\text{Cl})_2$), NaOH, and absolute ethanol of a reliable brand were used for this study. $\text{Zn}(\text{Cl})_2$ and $\text{Co}(\text{Cl})_2$ were taken according to the calculated stoichiometric ratio in a beaker containing absolute ethanol and were stirred for 2 h. NaOH mixed in ethanol was added to the chloride solution dropwise. The solution was then stirred at room temperature for 2 h. After 2 h, the precipitates were collected from the solution using centrifuge.

* Correspondence: saqlain007pk@hotmail.com

²Department of Physics, Forman Christian College (University), Lahore 54000, Pakistan

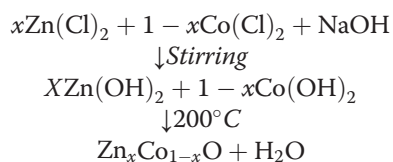
Full list of author information is available at the end of the article

The precipitates were washed several times using absolute ethanol and distilled water. Then, the precipitates were oven dried for 15 h. The product obtained at this stage was zinc and cobalt hydroxide powder.

Finally, the thermal decomposition of the zinc and cobalt hydroxide was used to obtain $Zn_xCo_{1-x}O$ nano-crystals. For this purpose, we placed them at temperature $200^\circ C$ for 6 h to obtain different sizes of nano-crystals. The chemical reaction is



The overall chemical reaction is revealed by given chemical equation:

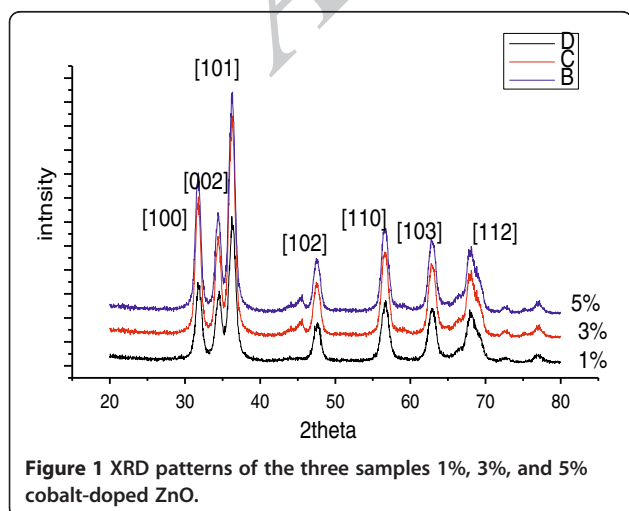


Characterization

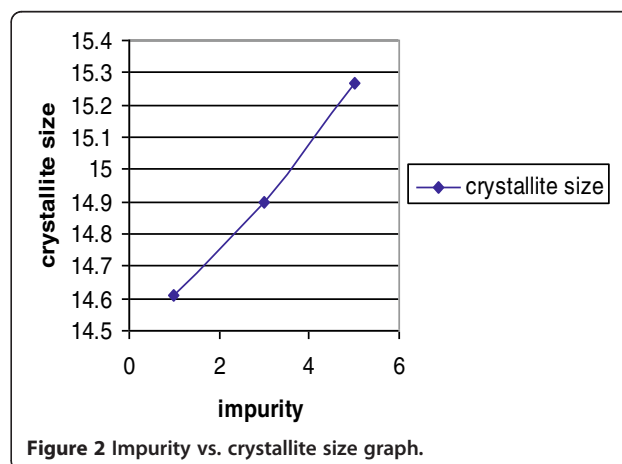
The X'Pert PRO MPD system of PANalytical Ltd. (Almelo, The Netherlands) was used for X-ray diffraction study. A simultaneous differential scanning calorimetry/thermo gravimetric analysis (DSC/TGA) system of SDT Q600 (TA Instruments, DE, USA) was used for thermogravimetric analysis. Lake Shore VSM 7407 (Lake Shore Cryotronics, Inc., OH, USA) was used for hysteresis studies. FTIR Bruker Tensor 27 (Bruker Daltonik GmbH, Bremen, Germany) was used to study absorbance properties.

Results and discussions

XRD graphs of doped ZnO nano-particles (shown in Figure 1) representing the standard picture of pure ZnO



even at higher doping concentrations show successful substitution of cobalt atoms with zinc atoms [8-10]. But the profiles of higher doping concentrations contain some additional peaks at $2\theta = 47^\circ$ which is a diffraction from the cobalt-crystal system. Although these peaks are very feeble, they exist and represent agglomeration of cobalt atoms at higher doping ratios. Distortion or other type of degradation (like shift of peaks and decrease of crystallinity) was not observed in doped samples as claimed by researchers working with Fe and Mn as dopants [11,12]. The crystallite size calculated using Scherer's formula was found to be 14.61, 14.9, and 15.27nm for 1%, 3%, and 5% (impurity vs. crystallite size graphically shown in Figure 2) cobalt-doped ZnO, respectively. A simultaneous DSC/TGA study of precursor was carried out during the fabrication of ZnO. DSC/TGA SDT Q600 measures amount and rate of change of mass as a function of temperature or time. Our DSC/TGA instrument is capable of performing both DSC and TGA simultaneously. DSC/TGA analysis was performed to study the change of phases during crystallization. The mixture of $Zn(OH)_2$ and $Co(OH)_2$ was taken before annealing and was put into the furnace of DSC in an inert environment. The simultaneous DSC/TGA graph is shown in Figure 3. The following results were deduced from the obtained data: Since the samples were fabricated in ethanol environment and then washed with distilled water and ethanol several times, the materials contain traces of ethanol. The first peak was observed at $57.45^\circ C$ which represents the mass loss due to evaporation of ethanol. This behavior can be observed from both heat flow and mass loss graphs. The second downward peak in heat flow graph and further decrease of mass was observed at $178.54^\circ C$ and $190.64^\circ C$ in weight curve, which represent decompositions of $Zn(OH)_2$ and $Co(OH)_2$, respectively. Both the materials liberate water molecules. Further, 10% mass loss was observed at



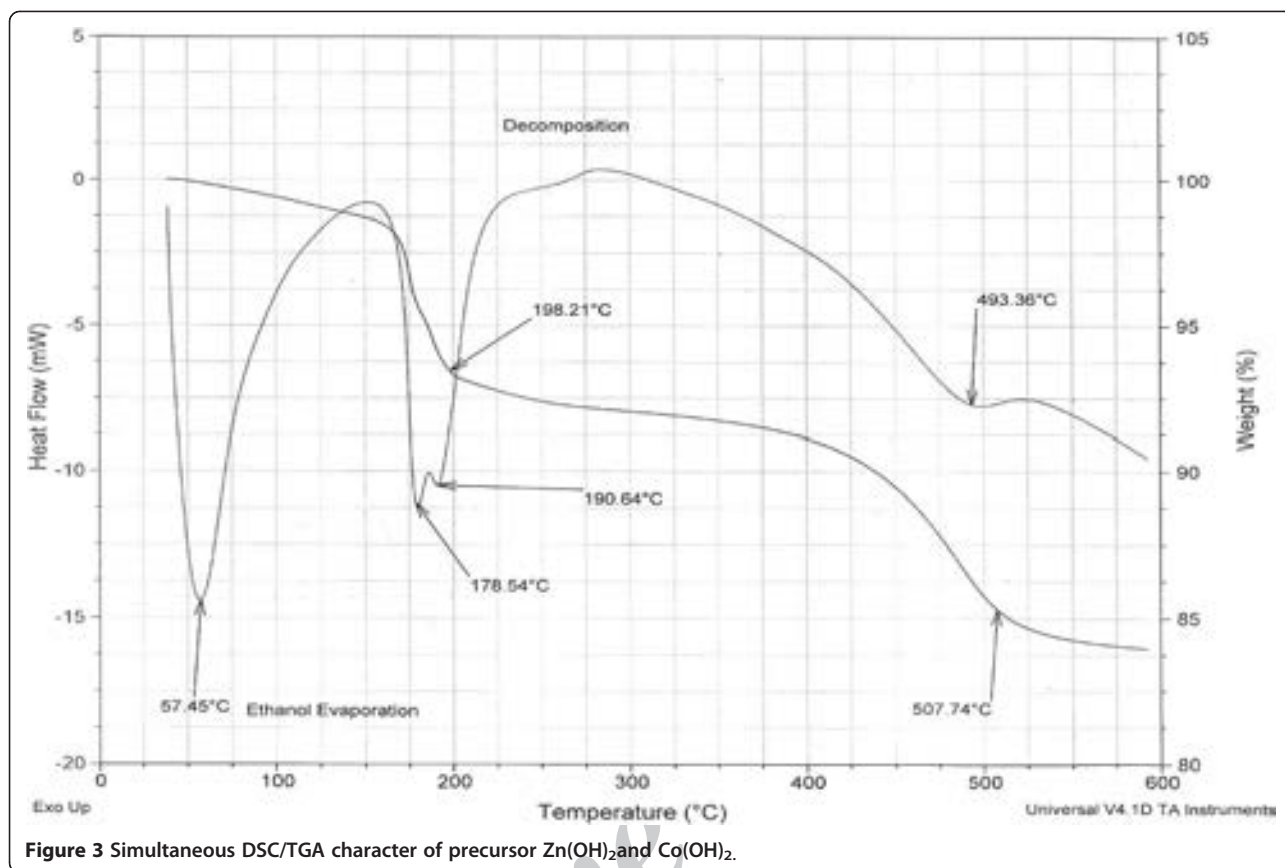


Figure 3 Simultaneous DSC/TGA character of precursor Zn(OH)₂ and Co(OH)₂.

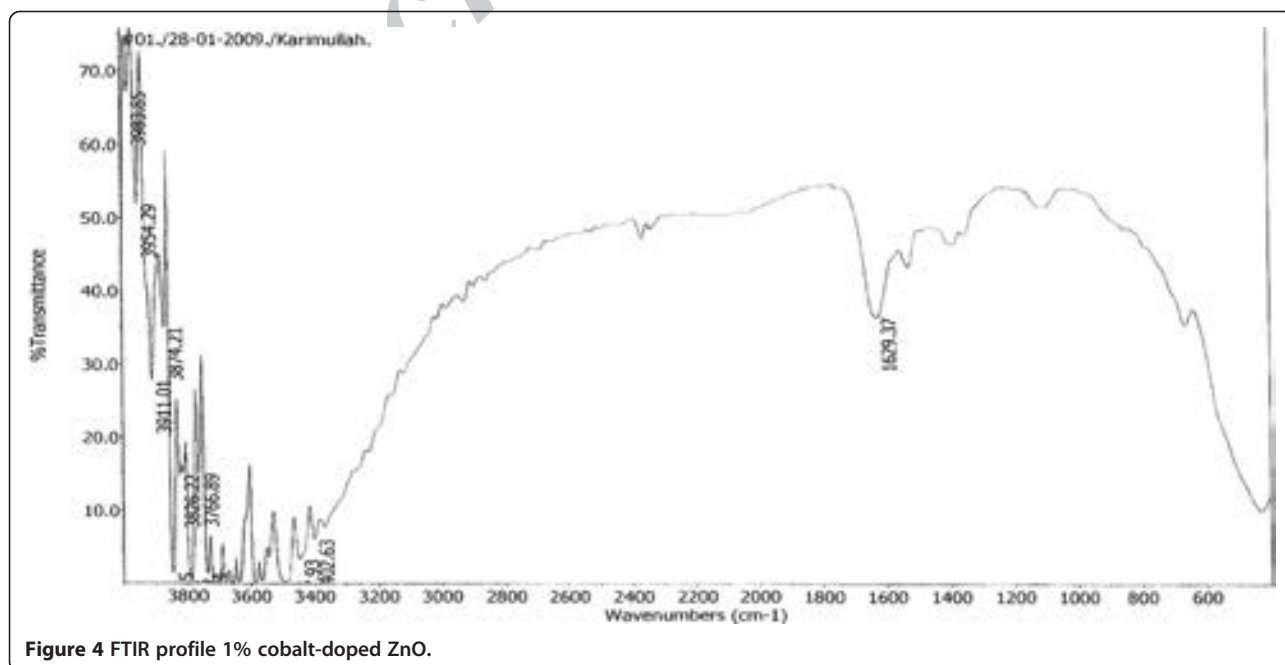
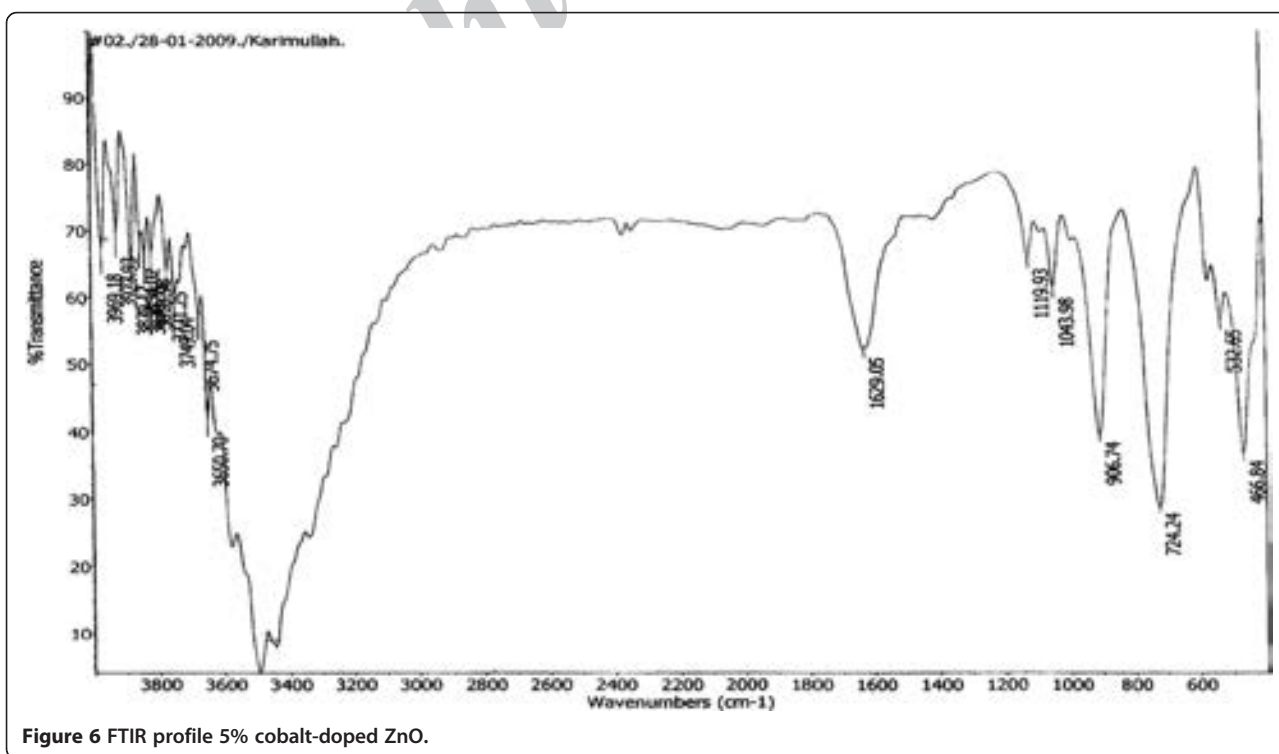
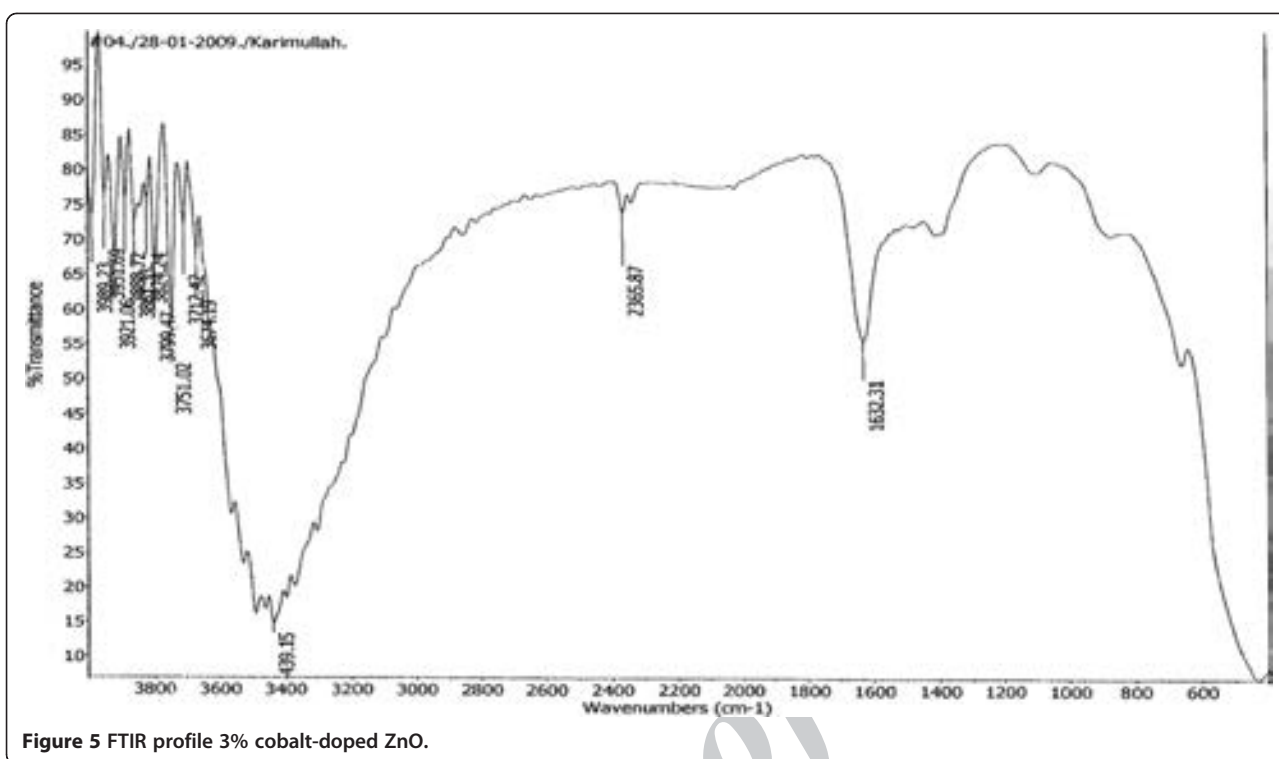


Figure 4 FTIR profile 1% cobalt-doped ZnO.



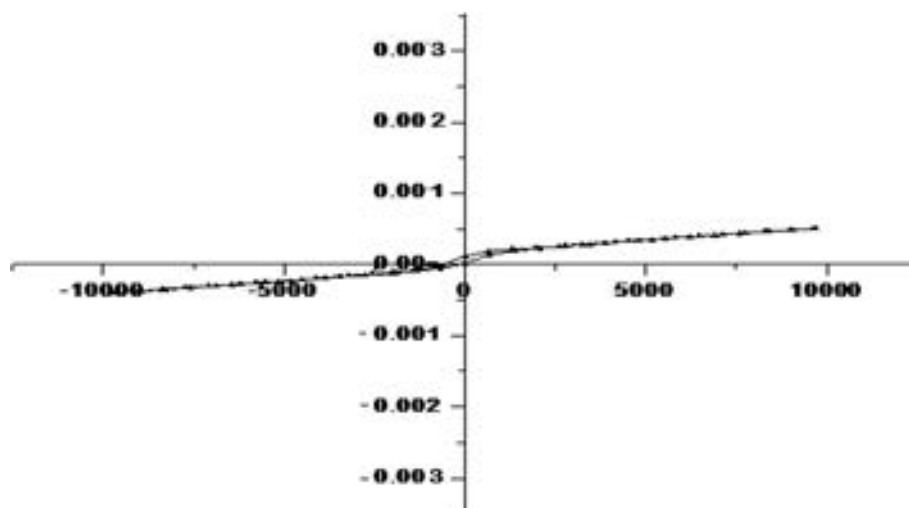


Figure 7 VSM profile of magnetic moment (emu) versus applied field (G) curve of 1% cobalt-doped ZnO.

approximately 500°C due to the evaporation of water of crystallization. These results were in good agreement with the literature [13]. The crystallization occurs during the removal of water molecules. So, heat loss during crystallization could not be observed from the heat graph because this heat is absorbed in the material to liberate water of crystallization. We can observe weight loss at 500°C and an endothermic peak of smaller intensity.

Fourier transformed infrared spectroscopy (FTIR), presented in Figures 4, 5, and 6, was performed to study the absorbance properties of fabricated samples and hence to deduce the nature of bonds present in the fabricated samples. In the given profile on wave number axis, the absorbance peaks from wave number 3,400 to 3,900 cm^{-1} are the peaks representing the hydroxyl (-OH) groups, which show incomplete removal of organic solvent. The next absorbance peak at wave number approximately 1,630 cm^{-1}

is due to the absorbance of organic group carbon (carbonyl carbon -C=O). The absorbance at wave number approximately 466 cm^{-1} is due to the typical bond between zinc and oxygen (Zn-O) [14-16]. The peaks from 700 to 900 cm^{-1} are attributed to the bond between cobalt and oxygen (Co-O) [17]. From the obtained FTIR profiles, we can observe the typical ZnO peaks and presence of organic contents in 1% and 3% doped samples, but in 5% cobalt-doped ZnO sample, we can observe additional peaks in wave number region 600 to 1,200 cm^{-1} which is the region of ZnO and Co-O bonding which again represents the presence of additional phases at higher concentration of doping.

We have done VSM analysis to observe magnetic characteristics of our fabricated samples to study room temperature ferromagnetism and the change in behavior of hysteresis curve by changing the magnetic doping

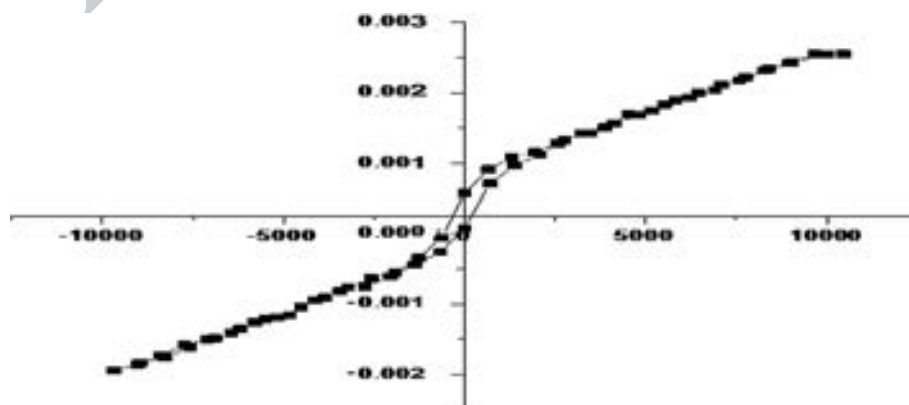


Figure 8 VSM profile of magnetic moment (emu) versus applied field (G) curve of 3% cobalt-doped ZnO.

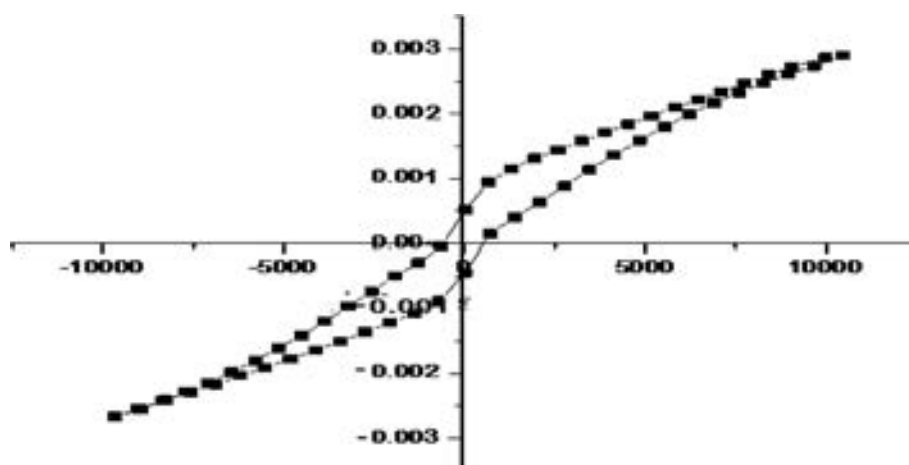


Figure 9 VSM profile of magnetic moment (emu) versus applied field (G) curve of 5% cobalt-doped ZnO.

concentration. The given Figures 6, 7, and 8 represent VSM profiles of Co-doped ZnO sketched at room temperature. Obtained profile confirms the presence of ferromagnetic behavior at room temperature and hence a successful doping where the impurity magnetic atom has successfully replaced the atoms of host crystal lattice, as XRD revealed pure ZnO at lower ratios. Presence of magnetic behavior depicts the presence of magnetic atoms. The smaller width of loop for 1% magnetic doping shows that it is a soft magnet, and 1% doped sample does not contain any cluster of atoms or segregation. So, we may deduce that presence of ferromagnetic behavior is due to intrinsic coupling between the atoms of doped materials but not due to the presence of secondary phase (segregation). We observed a proportional change in the shape and width of hysteresis loop, a stronger loop for 3% and 5%, as shown in Figures 8 and 9, doped samples. These results were again contrasting, where some researchers observed ferromagnetic ordering at lower doping concentration but paramagnetic behavior for higher doping concentration. For iron doping, it was explained that paramagnetic behavior is due to anti-ferromagnetic coupling at higher doping concentration [11,18-20]. In our cobalt-doped samples, a cobalt proportional ferromagnetic strength was observed due to different electronic configurations of cobalt and agglomeration of a little fraction of cobalt atoms (as revealed by XRD) which prevents anti-ferromagnetic coupling.

Conclusion

Different compositions of cobalt-doped ZnO nanocrystallites were successfully fabricated using co-precipitation method. For fabrication of Co-doped ZnO, decomposition temperature of precursor was determined by DSC/TGA analysis. XRD revealed standard ZnO

profile for lower doping but additional phases were present for higher doping. Similarly FTIR and VSM studies also revealed doping proportional properties.

Competing interest

The authors declare that they have no competing interests.

Authors' contributions

MAS is the prime investigator, performer, analyzer, and writer of the study. SAS performed the data analysis and proofreading, and to whom correspondence is addressed. MN has done the PH and atmosphere control. KR performed the FTIR analysis. RA provided the technical guidance. All authors read and approved the final manuscript.

Authors' information

All authors are experienced researchers of Materials Science and Nanotechnology. SAS and RA are PhD faculty members; the others are senior PhD students.

Acknowledgments

Authors would like to acknowledge the chairman of the Centre for Advanced Study in Physics, GC University Lahore, for providing funds, access to XRD, and for granting resources for VSM studies.

Author details

¹Department of Physics, GC University, Lahore 54000, Pakistan. ²Department of Physics, Forman Christian College (University), Lahore 54000, Pakistan. ³Pakistan Council of Scientific and Industrial Research (PCSIR), Lahore 54000, Pakistan.

Received: 8 October 2012 Accepted: 8 October 2012

Published: 29 October 2012

References

1. Bunn, CW: The lattice dimensions of zinc oxide. *Proc. Phys. Soc.* **47**, 836 (1935)
2. Damen, TC, Porto, SPS, Tell, B: Raman effect in zinc oxide. *Phys. Rev.* **142**, 570 (1966)
3. Decremps, F, Pellicer-Porres, J, Saitta, AM, Chervin, JC, Polian, A: High-pressure Raman spectroscopy study of wurtzite ZnO. *Phys. Rev. B.* **65**, 092101 (2002)
4. Özgür, U, Alivov, YI, Liu, C, Teke, A, Reshchikov, MA, Doğan, S, Vrutin, V, Cho, SJ, Morkoç, H: A comprehensive review of ZnO materials and devices. *J. Appl. Phys.* **98**, 041301 (2003)

5. Dietl, T, Ohno, H, Matsukura, F, Cibert, J, Ferrand, D: Zener model description of ferromagnetism in zinc-blende magnetic semiconductors. *Science* **287**, 1019 (2000)
6. Ohno, Y, Young, DK, Beshoten, B, Matsukura, F, Ohno, H, Awschallon, DD: Electrical spin injection in a ferromagnetic semiconductor heterostructure. *Nature* **402**, 790 (1999)
7. Pearton, SJ, Abernathy, CR, Overberg, ME, Thaler, GT, Norton, DP, Theodoropoulou, NA, Hebard, AF, Park, YD, Ren, F, Kim, J, Boatner, LA: Magnetization and structural studies of Mn-doped ZnO nanoparticles: prepared by reverse micelle method. *J. Appl. Phys.* **93**, 1 (2003)
8. Wang, J: Ultrafine ZnO powder prepared by precipitation/mechanical milling. *J. Mater. Sci.* **36**, 3273–3276 (2001)
9. Martiner, B, Sandiumenge, F, Fontcuberta, J: Ferromagnetism in Co-doped ZnO particles prepared by vaporization-condensation in a solar image furnace. *J. Magn. Magn. Mater.* **290**, 168–170 (2004)
10. Wang, Z, Zhang, H, Zhang, L, Yuan, J, Yan, S, Wang, C: Low temperature synthesis of ZnO nanoparticles by solid state pyrolytic reaction. *Nanotechnology* **14**, 11–15 (2003)
11. Caffarena, VD, Capitaneo, JL: Preparation of electrodeposited cobalt nanowires. *Mat. Res.* **9**(2), 205–208 (2006)
12. Xue, DB, Chen, JS, Zhou, TJ, Chow, GM: Effect of Mn-doping on temperature dependent magnetic properties of Li_1FeMnPt . *J. Appl. Phys.* **109**, 07B747 (2011)
13. Yang, H, Nie, S: Preparation and characterization of Co-doped ZnO nanomaterials. *Mater. Chem. Phys.* **114**, 279–282 (2009)
14. Jayakumar, OD, Gopalakrishnan, IK: Surfactant induced enhanced room temperature ferromagnetism in $\text{Zn}_{0.96}\text{Mn}_{0.03}\text{Li}_{0.01}\text{O}$ nanoparticles prepared by solid state pyrolytic reaction. *J. Cryst. Growth* **307**, 315–320 (2007)
15. Kim, HI, Choi, JM, Kim, DJ, So, MG: Synthesis and crystallization of fine SiC-Si₃N₄ composite powders by a vapor phase reaction. *J. Ceram. Proc. Res.* **3**(3), 146–149 (2002)
16. Sui, XM, Shao, CL, Liu, YC: White-light emission of polyvinyl alcohol/ZnO hybrid nanofibers prepared by electrospinning. *Appl. Phys. Lett.* **87**, 113–115 (2005)
17. Byrappa, K, Subramani, AK, Ananda, S, Lokanatha Rai, KM, Sunitha, MH, Basavalingu, B, Soga, K: Impregnation of ZnO onto activated carbon under hydrothermal conditions and its photocatalytic properties. *J. Mat. Sci.* **41**, 1355–1362 (2006)
18. Sharma, PK, Ranuk, DK, Avinash, PC: Effect of iron doping concentration on magnetic properties of ZnO nanoparticles. *J. Magn. Magn. Mat.* **321**, 2587–2591 (2009)
19. Ghule, K, Ghule, AV, Chen, BJ, Ling, YC: Preparation and characterization of ZnO nanoparticles coated paper and its antibacterial activity study. *Green Chem.* **8**, 1034–1041 (2006)
20. Ding, HM, Ding, J, Shi, Y, Liu, XY, Wang, J: Ultrafine ZnO powder prepared by precipitation/mechanical milling. *J. Mat. Sci.* **36**, 3273–3276 (2001)

doi:10.1186/2228-5326-2-31

Cite this article as: Shafique *et al.*: Effect of doping concentration on absorbance, structural, and magnetic properties of cobalt-doped ZnO nano-crystallites. *International Nano Letters* 2012 **2**:31.